Injection-locked coupled microstrip leaky-mode antenna array

C.-N.Hu and C.-K.C.Tzuang

Abstract: The paper presents a novel design for an injection-locked microstrip leaky-mode antenna array. It demonstrates that the coupling parameters can be obtained numerically, leading to the analysis of the steady-state phase relationships of the coupled oscillators based on Van der Pol equations for determining the excitation signals of the array. In particular, it applies the coupled-mode approach to investigating the clear and considerable mutual coupling effect on the radiation characteristics of the microstrip leaky-mode array. This, in turn, produces a very efficient and accurate assessment of the radiation far-field patterns. Finally, a proof-of-concept design using a two-element injection-locked microstrip leaky-mode array is presented for experimental verification, showing excellent agreement between theoretical data and measured results.

1 Introduction

Matured MMIC (monolithic microwave integrated circuit) and quasi-optical techniques offer the prospect of reducing construction costs for active phased arrays [1], making the application of such arrays a rapidly growing area of research [2–4]. However, the complexity of the distribution network required increases as the element number of the phased array system grows. Thus a challenge confronts us in designing the signal distribution for large phased array systems. Given the large size, high loss and dispersion in conventional transmission mediums, designers are seeking improved methods for high combination efficiencies using quasi-optical spatial power combining techniques [5, 6] and a simpler distribution network layout [7]. From this perspective, the microstrip leaky-mode antenna based array becomes attractive because it employs a linear array to achieve the pencil beam that otherwise can only be obtained by conventional two-dimensional arrays incorporating patch resonators or other means, greatly reducing component account. This paper describes a new design for beam scanning array based on the concept of quasi-optical power combining using the microstrip leaky-mode antenna array. As Fig. 1 shows, an injection signal from an external stable source feeds into one end of the active linear array with a unit element comprised of a free-running oscillator and a microstrip leaky-mode antenna. The injection signal couples into and locks the nearest active devices of the microstrip leaky-mode antenna. The latter then synchronises with the next sequential unit of the active antenna element, and so on. As the frequency of the external signal varies, the beam-scanning characteristic is derived from the nature of the leaky-wave antenna array.

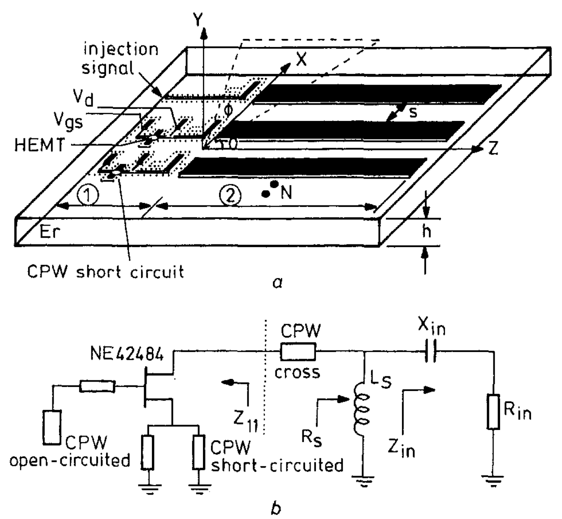

Fig. 1 *Generic, N-element injection locked microstrip leaky-mode antenna array, including CPW quasi-optical oscillators, CPW-to-slotline transitions, and slotlines for exciting EH_1 mode of individual microstrip lines, and simplified schematic diagram for antenna integrated with quasi-optical oscillator*
a Antenna array
b Schematic diagram of array integrated with oscillator
1 CPW (coplanar waveguide) quasi-optical oscillators on back side of substrate
2 Microstrip leaky-mode antennas with length *L*, width *W* and gap *S* on top side of substrate

2 Theoretical analysis

2.1 Mode coupling of complex-wave and coupling parameters

As Fig. 1 shows, microstrips are placed as close as possible to achieve sufficient coupling strength for an acceptable locking bandwidth. However, coupling between the adjacent microstrip lines alters the modal spectra of the microstrip's EH_1 mode, which is the first higher order of the microstrip mode leaking power away in the form of a space wave. By rigorous full-wave analysis [8], one can always obtain both the undisturbed (before coupled) EH_1 mode of a single microstrip line and all coupled EH_1 modes of the microstrip array with fewer elements. Fig. 2 plots the theoretical results of a 3-element array, clearly indicating the

IEE Proceedings online no. 20000599
DOI: 10.1049/ip-map:20000599
Paper first received 14th January and in revised form 20th April 2000
The authors are with the Institute of Electrical Communication Engineering, National Chiao Tung University, Hsinchu, Taiwan

effect of mode coupling of complex waves inherent in a microstrip leaky-mode array. The coupled-mode approach [9, 10] states that mode coupling of complex waves inherent in N-element leaky lines is governed by a system of linear differential equations and expressed as follows:

$$dI(z)_i/dz = -\gamma_i I_i(z) + \sum_{j=1}^{N} C_{ij} I_j(z) \qquad (1)$$

where $I_i(z)$ is the modal current vector on microstrip i and C_{ij} is the mutual coupling interaction between the ith and jth elements. Using matrix notation, eqn. 1 is abbreviated as

$$dI/dz = \bar{\bar{B}} \cdot \bar{I} \qquad (2)$$

where $\bar{\bar{B}} = [\mathrm{diag}(\gamma_i) - [C_{ij}]]$ and $\bar{I} = [I_1, I_2, ..., I_N]^t$. When all the coupled microstrips are in equal width, γ_i must be equal to γ, where γ is the complex propagation constant of the EH_1 leaky mode of a single microstrip. On the other hand, N coupled leaky-mode solutions should exist in the N-element array, denoted as $\lambda_1, \lambda_2, ..., \lambda_N$. For a specific mode with complex propagation constant λ_i, the modal solution mandates

$$d\bar{I}/dz = \gamma_i \cdot \bar{I} \qquad (3)$$

Substituting eqn. 3 into eqn. 2 for $i = 1, 2, ..., N$, we obtain

$$\bar{\bar{A}} \cdot \bar{I} = \bar{0} \qquad (4)$$

where $\bar{\bar{A}} = [\mathrm{diag}(\lambda) - \mathrm{diag}(\gamma_i) + [C_{ij}]]$. The source-free modal solutions require nontrivial solutions for the modal current vector $\bar{I}(z)$. Therefore eqn. 4 leads to a standard eigenvalue problem by solving

$$\det\left(\bar{\bar{A}}\right) = 0 \qquad (5)$$

Eqn. 4 clearly demonstrates that one can either attain the λ (coupled EH_1 modes) given $[C_{ij}]$ (the square matrix of coupling parameters) or deduce $[C_{ij}]$ given λ. Thus, substituting the rigorous data of the coupled EH_1 modes (λ shown in the solid line of Fig. 2) into eqn. 4, one can deduce all coupling parameters numerically. The Appendix (Section 8) carries out the detailed formulation for deducing all coupling parameters. By using eqn. 13, Fig. 3 plots the theoretical results of the coupling parameters C_{12} and C_{13}, revealing that the strength of C_{13} – coupling due to other-adjacent-element – is much smaller than that of C_{12}, nearest-neighbour coupling.

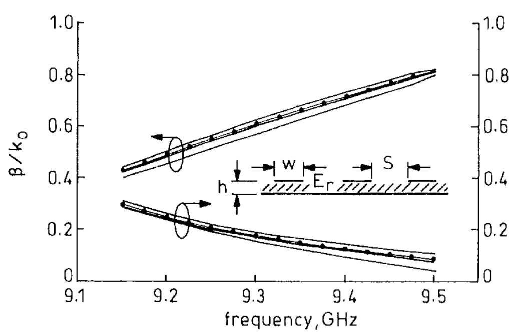

Fig. 2 *Comparison of dispersion characteristics of single microstrip line and those of 3-element coupled microstrip lines, showing that modal spectral of microstrip's EH_1 mode is altered by mutual coupling of adjacent lines*
—●— EH_1 mode of single microstrip line
- - - - coupled EH_1 modes of 3-element microstrip lines
w = 4.47mm, s = 10.765mm, h = 25mm, E_r = 10.2

2.2 Coupled oscillator theory

A competent theory of coupled oscillators needs to predict the steady-state phase relationships in the array numerically. York *et al.* [6] indicated that coupled Van der Pol equations adequately describe the coupled oscillator arrays for power combining. With predicted coupling parameters C_{ij} ($C_{ij} = \rho_{ij}\angle\Phi_{ij}$) by eqn. 13, the equations describing the amplitude and phase dynamics for an array of N elements can be achieved. From the theoretical results shown in Fig. 3, this work only considers the nearest-neighbour coupling, with $\rho_{ij} = 0$ for all $|i - j| \neq 1$. Furthermore, the coupling is reciprocal. Since the oscillators in the linear array are equidistant, all of the coupling terms are identical, and the following simplifications are possible: $\rho_{ij} \Rightarrow \rho$ and $\Phi_{ij} = \Phi$. Thus, one can (to first order) ignore the amplitude dynamics. The system is then described by [6] as follows:

$$\frac{d\theta_i}{dt} = \omega_i - \frac{\rho\omega_i}{2Q_i} \sum_{\substack{j=i-1 \\ j\neq i}}^{i+1} \frac{I_j}{I_i} \sin(\Phi + \theta_i - \theta_j) \qquad (6)$$

where $i = 1, 2, ..., N$, and where I_i is the instantaneous amplitude, ω_i is the free running frequency, and $\theta_i = \omega_i t + \phi_i$ is the instantaneous phase of oscillators i. Meanwhile Q is the Q-factor of the oscillator embedding circuits. Eqn. 6 allows the steady-state phase differences between each oscillator to be solved, given the free-running frequencies and computed coupling parameters by eqn. 13.

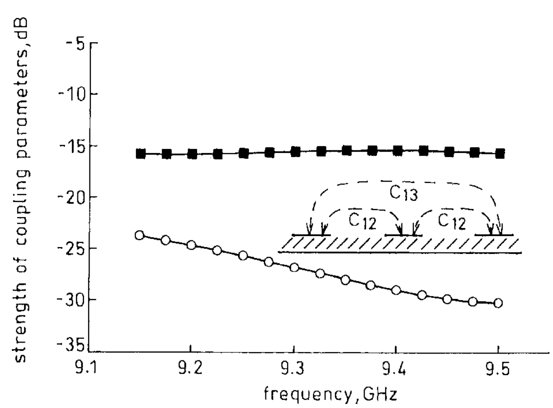

Fig. 3 *Strength of coupling parameters ($10\log|C_{1i}|$, i = 2, 3), showing that coupling parameters other than nearest-neighbour lines (C_{12}) can be ignored as negligible*
-■- C_{12} -○- C_{13}
w = 4.47mm, s = 10.765mm, h = 25mm, E_r = 10.2

2.3 Radiation pattern of an active, coupled, microstrip leaky-mode array

For a coupled microstrip array, each coupled EH_1 mode is supported by a particular modal current distribution on the strips. This can be viewed as an eigenvalue corresponding to a specified eigenvector. For instance, another view for distinguishing the two leaky modes of a two-element array is based on the eigenvectors of the modal current distributions on the strips, either in-phase ($[1/\sqrt{2}, 1/\sqrt{2}]$) for the EH_1 even-mode or out-of-phase ($[1/\sqrt{2}, -1/\sqrt{2}]$) for the EH_1 odd-mode. These in-phase and out-of-phase modal current distributions are two orthogonal eigenvectors of the two-element microstrip array from the perspective of the coupled-mode approach. Thus the excitation signal ($\bar{I}^{inc}(0)$), which is obtained by eqn. 6 provided that active devices oscillate equal amounts of instantaneous amplitude (I_i), may be expressed by superposition of N eigenvectors based on the eigenfunction approach, i.e.

$$\bar{I}^{inc}(0) = \sum_{i=1}^{N} a_i \bar{\xi}_i \qquad (7)$$

where $\bar{I}^{inc}(0)$ is the oscillating signal on the $z = 0$ plane, $\bar{\xi}$ is the eigenvector of $[A]$, and a_i represents the modal amplitude of the ith coupled EH_1 mode. Thus, applying Huygen's principle to an equivalent current distribution travelling along the microstrip makes it possible to obtain the far-zone electric fields of the kth microstrip with a length of L [11] expressed as follows:

$$E_r \simeq E_\theta \simeq 0 \tag{8a}$$

$$E_\phi^k \simeq -jE_o \frac{he^{-jkr}}{\pi r} \times \left\{ \sin\theta \left[\frac{\sin(\Omega)}{\Omega}\right] \sum_{i=1}^{N} a_i \xi_{ik} \left[\frac{e^{Z_i L} - 1}{Z_i}\right] \right\} \tag{8b}$$

where

$$\Omega = kh \sin\theta \cos\phi \tag{8c}$$

$$Z_i = j(\cos\theta - \beta_i) - \alpha_i \tag{8d}$$

$$k = 2\pi/\lambda_o \tag{8e}$$

where λ_o is the free-space wavelength, β_i (α_i) is the phase (attenuation) constant of the ith coupled EH_1 mode and ξ_{ik} represents the kth element at the ith eigenvector. Meanwhile, the total far-zone electric field E_ϕ^T is the superposition of the N-element microstrip leaky-mode array expressed as

$$E_\phi^T = \sum_{k=1}^{N} E_\phi^k \exp(jkx_k \cos\theta \cos\phi) \tag{9}$$

where x_k is the location of the kth microstrip. Thus, the radiation characteristics of the coupled microstrip array can be simulated by the following procedures:

(a) Solving the coupled EH_1 modes of a three-element array by using rigorous full-wave analysis makes it possible to deduce the coupling parameters using eqn. 13.

(b) Substituting the computed coupling parameters (step (a)) into the characteristic equation of $[A]$ in eqn. 4 allows the computation of all the coupled EH_1 modes (λ_i, i = 1, 2, ..., N) and their corresponding eigenvectors ($\bar{\xi}_i$, i = 1, 2, ..., N) by solving the standard eigenvalue problem (eqn. 5).

(c) By substituting computed coupling parameters (in step (a)) into eqn. 6, we can solve the steady-state phase difference (θ_i) between oscillators for an empirically determined Q-factor to obtain $\bar{I}^{inc}(0)$.

(d) With computed $\bar{I}^{inc}(0)$ and $\bar{\xi}_i$, we obtain N excited modal amplitudes (a_i, i = 1, 2, ..., N) by solving N linear independent equations derived by eqn. 7.

(e) Substituting computed values of a_i, λ_i and $\bar{\xi}_i$ into eqn. 8 makes it possible to simulate the far-field pattern of the injection-locked microstrip leaky-mode array.

3 Proposed proof-of-concept design of a two-element active array

3.1 Antenna design

A two-element microstrip leaky-mode antenna array integrated with a quasi-optical oscillator presents the prototype of a proof-of-concept design. The slotline underneath the microstrip is employed to excite the EH_1 mode efficiently [8], and also acts as a short-circuited tuning stub to compensate for the imaginary part of the input impedance of the antenna. Thus, an L-type matching circuit is established in a very compact fashion. Followed by a CPW-to-slotline transition, the slotline is transformed into a CPW (coplanar waveguide) line to integrate with a quasi-optical oscillator. Fig. 1b shows the single antenna impedance matching scheme described above.

Realising the compact antenna design (as Fig. 1b shows) needs the quantitative assessment of the characteristic impedance for the microstrip leaky mode to provide an insightful circuit-domain view of the leaky line. The input impedance of the microstrip leaky-mode antenna with length L is expressed as

$$Z_{in}(\omega) = -jZ_c(\omega)\cot(k_z L) \tag{10}$$

where Z_c is the characteristic impedance of the microstrip leaky mode given by [12, 13] as

$$Z_c = \frac{1}{2}\int_S \vec{E} \times \vec{H}^* \cdot \hat{z}da \bigg/ |I_t|^2 \tag{11}$$

where I_t is the total current on the metal strip, and S is the cross-sectional area of the microstrip. It is well known that the leaky line exhibits nonstandard growing behaviour along the transverse plane, resulting in invalid computation of Poynting power. Das [12] reported the method for obtaining the leaky-mode characteristic impedance by decomposing the transverse fields into bound fields and leaky fields and considering bound fields only for Poynting power computation. Applying this definition, the characteristic impedance of the microstrip leaky mode can be computed by using the 2-D integral equation method [13]. Fig. 4 plots the theoretical results of the input impedance for this particular design, where the solid line (dashed line) represents the real (imaginary) part of the input impedance for the microstrip leaky-mode antenna of length 145mm. With Z_{in} (92.135 – j16.36Ω) computed at the desirable frequency of 9.4GHz, the value of shunt inductance (Ls) can be calculated based on circuit theory so that the microstrip leaky-mode antenna is matched to the slotline impedance of R_s (95Ω). The calculated values of R_s and L_s allow the dimensions of the slotline of width 15mm and length 142mm to be determined.

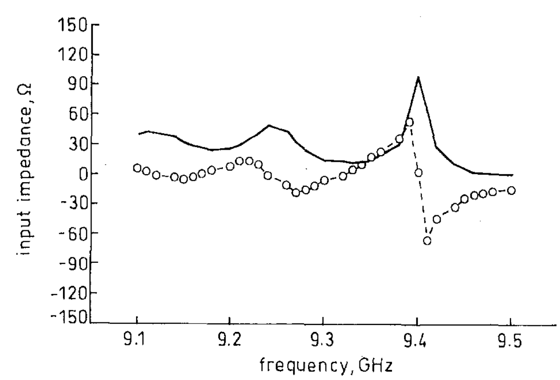

Fig. 4 *Theoretical input impedance of a single microstrip leaky-mode antenna as computed by 2-D spatial-domain integral equation method [13]*
—— Z_{in} (real) O-- Z_{in} (imaginary)
w = 4.47mm, L = 145mm, h = 25mm, E_r = 10.2

3.2 Quasi-optical oscillator design

Various oscillator designs share similar design procedure regardless of the problem being solved. We first employ linear analysis to obtain the first-order design parameters of the proposed circuit schematic diagram as shown in Fig. 1b and then apply harmonic balance analysis to predict the oscillation frequency and to optimise the output power. The simulation result indicates the first harmonic at a frequency of 9.403GHz with power level of 12.44dBm. The quasi-optical oscillator was optimised to maximise power output for the desirable pointing direction of the leaky-mode antenna. The complete quasi-optical oscillator was built on a 25mm-thick RT/Duroid 6010 substrate with a relative dielectric constant of 10.2. For a free-running situation, the near-field pick-up measurement shows that the unlocked source oscillates at 9.415GHz with 11.8dBm power level, which is very close to the simulated result. Meanwhile, the measurement also observes DC-to-RF efficiency of 23% and phase noise of –90dBc/Hz at a 10kHz offset from the carrier.

4 Measurement results

The theoretical prediction of the coupling parameters for the leaky-mode antenna array was first validated experimentally using an imaging technique [6]. A single active microstrip leaky-mode antenna was tuned to a measured free-running frequency of 9.415GHz; the microstrip leaky-mode antenna was then positioned near a vertical ground plane, thus simulating two identical, in-phase (for the odd-symmetrical nature of the microstrip EH_1 mode) coupled oscillators. With varying position of the microstrip leaky-mode antenna, a frequency shift was evident which relates to the coupling parameters. Fig. 5 displays the results, and indicates that the theoretical prediction by this approach and by the empirically determined Q-factor of 14.1 compares very favourably with array measurement. Subsequently a prototype, two-element, active array was built for experimental validation.

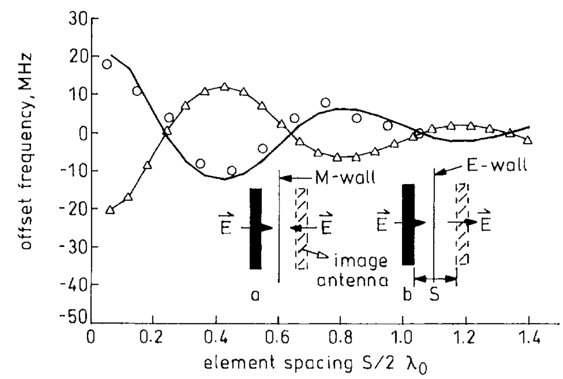

Fig. 5 *Measured frequency shift against active leaky-mode antenna separation*
X-band microstrip leaky-mode antenna integrated with a quasi-optical oscillator
λ_0 is the wavelength in free space corresponding to frequency of 9.415GHz
△ out-of-phase coupling —— in-phase coupling
○ measured data
a Out-of-phase coupling; *b* in-phase coupling

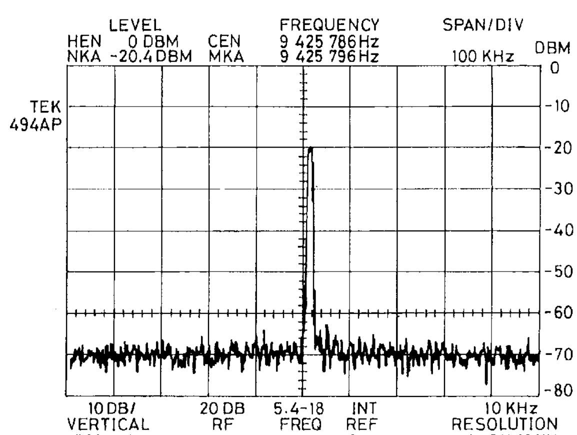

Fig. 6 *Near-field power spectrum of injection locked oscillator synchronised to 9.426GHz*

For a free-running situation, the near-field pick-up measurement shows that the unlocked source oscillates at 9.415GHz with 11.8dBm output power. Then, an injection locking measurement is taken. As an external stable source of 12dBm at 9.426GHz is injected into one end of the array, the oscillator is locked and synchronised to the frequency of the injection signal through the mutual-coupling interaction between antennas. Fig. 6 shows the spectrum of an injection-locked oscillator, demonstrating 23MHz locking ranges. Furthermore, the measured ERP (effective radiated power) of a single- and two-element array is 22.5dBm and 27.3dBm, respectively. Fig. 7 (Fig. 8) plots the measured far-field pattern in the azimuth (elevation) plane cut at the peak value of the main lobe as a comparison with ones by using the rigorous analysis described in Section 2, and good agreement is achieved. As the frequency of the external source sweeps, the antenna will simultaneously scan it by phase control in azimuth and by frequency control in elevation. Fig. 9 plots the measured far-field patterns in the azimuth plane (x-y plane) cut at the peak value of the main beam corresponding to the injected frequencies at 9.406, 9.410 and 9.415GHz, respectively. The antenna beam is scanned to ϕ/θ_{EL} (x-y plane/y-z plane) equal to 4.6°/44.5°, 15.3°/40.9° and 17.5°/36.7°, respectively, as the injected frequency changes from 9.406 to 9.415GHz. The theoretical prediction of the beam scanning direction points towards ϕ/θ_{EL} (x-y plane/y-z plane) at 3.9°/43.9°, 13.4°/41.4° and 19.5°/39.2° for the respective injection signal frequencies, showing good agreement with measured results.

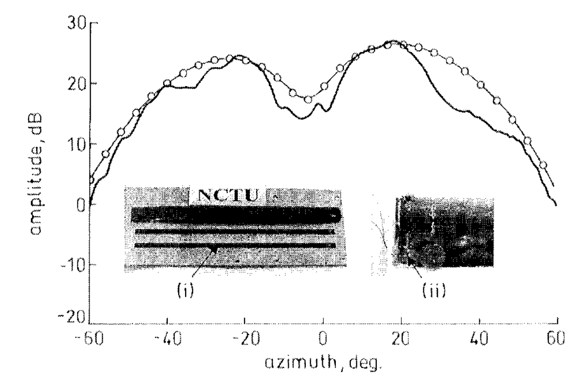

Fig. 7 *Comparison of measured and simulated far-field patterns in azimuth plane (x-y) cut at peak value of main lobe*
Inset photograph is prototype of experimental two-element microstrip leaky-mode array integrated with one quasi-optical oscillator
-○- simulated —— measured; frequency = 9.415GHz
(i) microstrip leaky-mode antenna on top side
(ii) CPW oscillator on back side

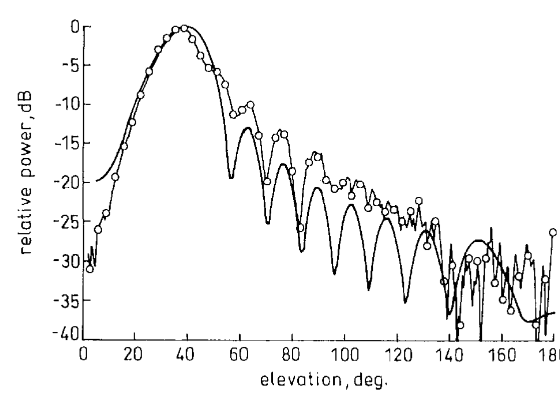

Fig. 8 *Comparison of measured and simulated far-field patterns in elevation plane (y-z) cut at peak value of main lobe*
—— this approach ○ measured; frequency = 9.415GHz

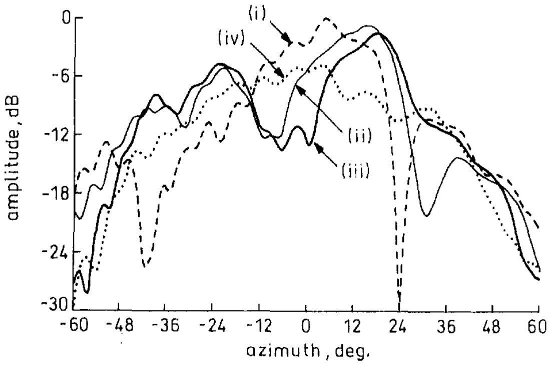

Fig. 9 *Measured far-field beam scanning patterns controlled by frequencies of injection signal*
F = (i) 9.406GHz; (ii) 9.41GHz; (iii) 9.415GHz; (iv) 9.41GHz (single element)

5 Conclusion

This work has presented an injection-locked microstrip leaky-mode antenna array in which beam scanning has been achieved without using dedicated phase shifters. The coupled-mode approach is adopted to analyse and design an injection-locked coupled microstrip leaky-mode antenna array that considers the mutual coupling of the leaky lines. Finally, this study experimentally verifies the novel design via a two-element, proof-of-concept design, exhibiting 23MHz locking bandwidth, 27.3dBm ERP and one-sided continuous H-plane beam scanning from 5° to 17° for 10MHz offset from the free-running frequency of 9.415GHz.

6 Acknowledgement

The authors would like to thank Dr. G.J. Chou and S.D. Chen for their helpful discussion. This work was supported by National Council of the ROC under grant NSC 88-2213-E009-073 (-101).

7 References

1 SEEDS, A.J., BLANCHFLOWER, I.D., GOMES, N.J., KING, G., and FLYNN, S.J.: 'New developments in optical control techniques for phased array radar', IEEE MTT-S Symp. Digest, 1988, pp. 905–908

2 DARYOUSH, A.S.: 'Optical synchronization of millimeter-wave oscillators for distributed architectures', *IEEE Trans.*, 1990, **MTT-38**, (3), pp. 467–476

3 LIAO, P., and YORK, R.A.: 'A six-element beam-scanning array', *IEEE Microw. Guid. Wave Lett.*, 1994, **4**, (1), pp. 20–22

4 STEPHAN, K.D.: 'Inter-injection-locked oscillators for power combining and phased arrays', *IEEE Trans.*, 1986, **MTT-34**, (10), pp. 1017–1025

5 YORK, R.A., and COMPTON, R.C.: 'Quasi-optical power combining using mutually synchronized oscillator arrays', *IEEE Trans.*, 1991, **MTT-39**, (6), pp. 1000–1009

6 YORK, R.A., and COMPTON, R.C.: 'Measurement and modeling of radioactive coupling in oscillator arrays', *IEEE Trans.*, 1993, **MTT-41**, (3), pp. 438–444

7 SEEDS, A.J.: 'Optical control of microwave devices'. Proceedings of SBMO international Microwave symposium, Campians, Brazil, 1985, pp. 308–311

8 CHOU, G.-J., and TZUANG, C.-K.C.: 'An integrated quasi-planar leaky-wave antenna', *IEEE Trans.*, 1996, **AP-44**, (8), pp. 1078–1085

9 HAUS, H.A., and HUANG, W.: 'Coupled-mode theory', *IEEE Proc.*, 1991, **79**, (10), pp. 1505–1518

10 TZUANG, C.-K.C., and HU, C.-N.: 'The mutual coupling effects in large microstrip leaky-mode array'. IEEE MTT-S Symp. Digest, Baltimore, USA, 1998, pp. 1791–1794

11 CHOU, G.-J., and TZUANG, C.-K.C.: 'Oscillator-type active-integrated antenna: the leaky-mode approach', *IEEE Trans.*, 1996, **MTT-44**, (12), pp. 2265–2272

12 DAS, N.D.: 'Power leakage, characteristics impedance, and leakage-transition behavior of finite-length stub sections of leaky printed transition lines', *IEEE Trans.*, 1996, **MTT-44**, (4), pp. 526–536

13 TZUANG, C.-K.C.: 'Leaky mode perspective of printed antenna'. Proceedings of 1998 Asia-Pacific Microwave conference, 1998, pp. 1471–1478

8 Appendix: Formulation of coupling coefficients

Roots of the characteristics polynomial function of $\bar{\bar{A}}$ are essentially the complex propagation constants for the coupled microstrips array. Thus we can rewrite eqn. 5 as

$$\det\left(\bar{\bar{A}}\right) = \lambda^N + b_{N-1}\lambda^{N-1} + \cdots + b_1\lambda^1 + b_{01} = \prod_{i=1}^{N}(\lambda - \lambda_i) \tag{12}$$

where λ_i (i = 1–N) are eigenvalues to be solved and b_i (i = 1–N) are the constant coefficients which are a function of the 'undisturbed' leaky mode (γ) and coupling coefficients (C_{ij}). Expanding the determinant ($\det(\bar{\bar{A}})$), and comparing order by order at both sides of eqn. 12 for N = 3, we obtain the following equations for solving the known coupling C_{12} and C_{13}, representing the coupling parameters of adjacent and other-than-adjacent elements, respectively:

$$\begin{cases} \gamma = (\lambda_1 + \lambda_2 + \lambda_3)/3 \\ \gamma^3 - 2C_{12}^2 C_{13} - \left(2C_{12}^2 + C_{13}^2\right)\gamma = \lambda_1\lambda_2 + \lambda_2\lambda_3 + \lambda_1\lambda_3 \\ 3\gamma^2 - 2C_{12}^2 - C_{13}^2 = \lambda_1\lambda_2\lambda_3 \end{cases} \tag{13}$$